Catalysis Communications 56 (2014) 115–118

Contents lists available at ScienceDirect

Catalysis Communications

journal homepage: www.elsevier.com/locate/catcom

Short Communication

Evaluation of gold-decorated halloysite nanotubes as plasmonic photocatalysts

Leyre Gómez [a,b,d], José L. Hueso [a,b,d,*], M. Carmen Ortega-Liébana [a,b,d], Jesús Santamaría [a,b,d], Stephen B. Cronin [c,e,f]

[a] Institute of Nanoscience of Aragon (INA), University of Zaragoza, Zaragoza 50018, Spain
[b] Networking Research Centre of Bioengineering, Biomaterials and Nanomedicine (CIBER-BBN); C/ Monforte de Lemos, 3-5, Pabellón 11, 28029, Madrid (Spain)
[c] Department of Chemistry, University of Southern California, Los Angeles, CA 90089, USA
[d] Department of Chemical Engineering and Environmental Technology, University of Zaragoza, Zaragoza 50018, Spain
[e] Department of Electrical Engineering, University of Southern California, Los Angeles, CA 90089, USA
[f] Department of Physics, University of Southern California, Los Angeles, CA 90089, USA

ARTICLE INFO

Article history:
Received 3 June 2014
Received in revised form 9 July 2014
Accepted 11 July 2014
Available online 17 July 2014

Keywords:
Gold nanoparticles
Plasmonics
Organic contaminant
Photocatalysis
Halloysite

ABSTRACT

Herein we report on the synthesis of gold-decorated halloysite nanotubes (HNTs) and their evaluation as photocatalysts in the degradation of a model organic contaminant. The combination of photo-thermally-induced local heating and charge transfer mechanisms between the nanostructured gold surface and the organic molecule results in the observed dye decomposition. The use of an inexpensive natural clay support with suitable surface chemistry and adsorption properties represents an eco-friendly method for light-induced oxidation reactions carried out at ambient temperatures.

1. Introduction

The search for alternative strategies for conventional thermally-driven catalytic processes represents a scientific challenge of increasing interest. Greener routes involving more efficient reactors and the use of naturally available sources have boosted the research on photo-catalysts able to drive chemical reactions in the presence of UV–Visible light. The most extended group of photocatalysts is based on semiconductor materials such as TiO_2 or ZnO, that are able to generate electron–hole pairs in their conduction and valence bands respectively and form reactive radicals for secondary processes [1,2]. In order to improve their photocatalytic activity or shift their efficiency towards the visible spectrum, different hybrid structures containing noble-metal nanocrystals or nanostructured quantum dots have been also successfully evaluated [3–7]. These nanostructured materials decorated onto photo-active semiconductor supports are used as photo-sensitizers that enhance the electron–hole pair's lifetime and the electron-transfer phenomena occurring at the nanoparticle–semiconductor interface.

Nevertheless, a renewed attention is currently being paid to the direct photo-catalytic effect of noble-metal nanoparticles [7–14]. Several activation mechanisms have been proposed to justify their photo-active nature without incurring into the same photo-catalytic principles applied to semiconductors. The most extended so far involves the so-called Surface-Plasmon-Resonant (SPR) effect [15]. This SPR effect occurs when metal nanoparticles strongly absorb light at certain wavelengths (normally in the visible-NIR range) and the electromagnetic field of the incident light couples with the oscillation of the conduction electrons present in the metal nanoparticles. The SPR absorption may cause rapid heating of the nanoparticles when the electrons return to their basal states and release heat to the lattice and the surroundings [16]. This photo-thermal effect may strongly enhance reaction rates and selectivities. A second enhancement mechanism based on the injection of electrons into the unoccupied molecular orbitals of the targeted molecules has been also suggested and is currently under investigation [10].

In this work, we present a rationalized synthesis of gold-decorated halloysite nanotubes (HNTs) and their evaluation as photocatalysts. We prove that a careful selection of gold nanoparticle sizes is required to match the resonant frequency of the incident green laser. In addition, an efficient distribution of the gold nanoparticles deposited onto the HNTs is crucial to promote the photo-decomposition of the dye. Moreover, the HNTs, naturally occurring aluminosilicates with $[Al_2Si_2O_5(OH)_4 \cdot nH_2O]$ nominal composition and a representative morphology where silica tetrahedrons and alumina with octahedral structure form hollow nanotubes are presented as a readily available

* Corresponding author.
E-mail addresses: jlhueso@unizar.es (J.L. Hueso), scronin@usc.edu (S.B. Cronin).

http://dx.doi.org/10.1016/j.catcom.2014.07.017
1566-7367/

and inexpensive support with suitable surface chemical composition for the attachment of nanoparticles.

2. Results and discussion

The amine-grafting of the halloysite nanotubes and the subsequent gold seeding process were confirmed by TEM as depicted in Fig. 1a–b (see Supporting information for further synthesis details). The electrostatic attraction between positively charged amine terminal groups and negatively charged Au NPs, especially at low pH values, favored a suitable coating and distribution of the pre-formed metal nanoparticles. The Au NPs were synthesized in advance with the aid of THPC as reducer and stabilizer [17,18] and the amination of the tubular clay support was carried out under mild conditions using a simple flask without any especial precaution with air or humidity, since inert conditions did not render a better anchoring of Au NPs despite possible self-polymerization events of APTES. Further details on the synthesis are fully described in Supplementary information and in previous works [19,20].

Fig. 1c shows the SPR absorption band for both Au-HNT samples centered at ca. 530 nm. Therefore, the optical maximum absorption of the catalysts perfectly matched with the incident green laser wavelength (532 nm) used in the photocatalytic experiments. The average diameter of the pre-formed Au NPs was ca. 5.3 ± 1.6 nm for the catalyst with 2% loading (see inset in Fig. 1a) and slightly higher for the HNTs with 4.2 wt.% Au (6.2 ± 2.7 nm; see inset in Fig. 1b). The main differences were based on the gold size distribution along the HNT support (see Fig. 1a–b). The HNTs with 4.2 wt.% Au loading contained bigger agglomerates of nanoparticles and wider size dispersions, thereby coinciding with the partial broadening of the SPR band observed in Fig. 1c.

Both Au-HNT samples with different gold loadings and their respective control experiment in the absence of catalyst were tested for the degradation of Methyl Orange (MO) as organic contaminant, under different laser irradiation intensities. As shown in Fig. 1d, only the sample with 2 wt.% Au content increased the MO decomposition rate as the laser intensities increased from 0.2 to 2 W. A 16-fold enhancement of the MO degradation was observed at the maximum power in comparison with control conditions (Fig. 1d). The Au-HNT sample with 4.2 wt.% Au slightly decreased the initial MO concentration by only 4% at the maximum applied power of 2 W (see Fig. 1d). Additional experiments under similar experimental conditions were performed using different excitation sources such as a red laser (633 nm) and an UV Hg lamp with two bandpass filters at 254 and 365 nm, respectively. The absence of dye degradation further corroborated the plasmon-enhanced photocatalytic effect of the Au-HNTs when the SPR maximum absorption and the incident laser wavelength overlapped (green laser conditions).

The light-driven degradation mechanism of MO can be partly ascribed to thermal heating effects induced by the resonant excitation of the plasmonic electrons in the Au NPs. This resonating oscillation coupled with the incident low-power laser wavelength is converted into lattice vibrations and finally released as heat [16]. This principle has been previously observed for gold nanoparticles in phototherapy and remotely photo-triggered heating release experiments [19,21]. Moreover, the plasmon-mediated oxidation of carbon monoxide [22],

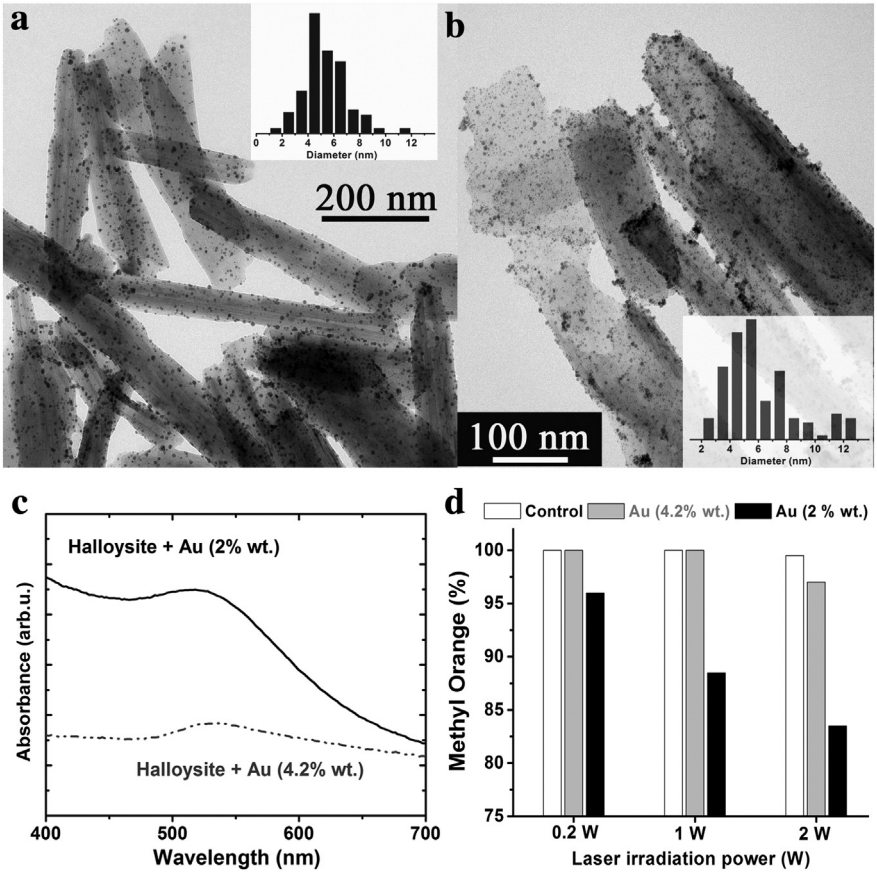

Fig. 1. TEM images corresponding to the amine-functionalized halloysite nanotubes after the seeding step with gold nanoparticles prepared with different volumes of the initial 1 wt.% $HAuCl_4$ salt precursor (see Section 2 for details). a) HNTs with 2 wt.% Au loading (inset includes the Au NP size distribution centered at 5.3 ± 1.6 nm); b) HNTs with 4.2 wt.% Au loading (inset refers to the Au NP size distribution centered at 6.2 ± 2.7 nm); c) UV–Vis spectra of the Au-HNT catalysts with different Au loadings; d) degradation of Methyl Orange in the absence (white column) and the presence of the Au-HNT catalysts under different laser irradiation power values (concentration of catalysts: 0.5 g L^{-1}; concentration of dye: 20 mg L^{-1}; volume of reaction: 1 mL; irradiation time: 1 h).

Volatile Organic Compounds (VOCs) [6] or ethanol [16] has been successfully tested and predominantly attributed to induced photo-thermal effects. Likewise, other reactions carried out in organic media for the selective production of fine chemicals have taken advantage of the rapid increase of temperature in the Au NP surfaces to overcome activation energy barriers and accelerate reaction rates without the need of external heating sources [23].

In addition, other tentative reaction pathways based on charge transfer mechanisms have been also proposed for the plasmon-induced photo-catalytic degradation of organic dyes and alternatively for selective photo-oxidation of gas-phase [24,25] and liquid-phase reactions [5,7–9,11–14,26,27]. In this latter mechanism, it is claimed that after the SPR absorption and subsequent intraband excitation of 6sp electrons, the newly generated positive charges are rapidly neutralized after retrieving electrons (oxidizing) from the surrounding organic molecules. Therefore, the energetic electrons in the 6sp band can further react with molecular O_2, yielding O_2^- species that subsequently react to form other active radical species [5,9]. Alternatively, it has been also suggested that dye molecules can be sensitized and polarized under the laser irradiation and inject additional electrons to facilitate the formation of O_2^- species, especially if multiple absorption phenomena take place under laser irradiation [5,9,28,29].

In our opinion, the photo-catalytic enhancement observed for the Au-HNTs is based on a combination of both mechanisms: (i) Photo-enhanced electron–hole pairs are preferentially formed at the SPR absorption wavelengths; (ii) the MO dyes adsorbed onto the support and nearby the gold surfaces are further sensitized and polarized; and (iii) hot electrons from Au NPs are injected to form highly reactive radical species. The activation barrier for these processes is overcome by the locally induced photo-thermal effect at the SPR absorption wavelength. If the process were light-induced only, as proposed by Zhu et al. [5,9] an additional degradation rate would have been detected upon exposure to an UV irradiation source and it did not occur under our experimental conditions. Therefore, the influence of the SPR photo-thermally induced heating at local levels must be fully taken into account, not as the main controlling mechanism but as the initial step for subsequent charge transfer processes. Hence, the negligible degradation of MO in the sample containing a higher gold content and a major number of aggregated particles (Fig. 1b) was also indicative of the importance to have a good Au NP dispersion to ensure a good contact between the active sites of the noble-metal nanoparticles and the adsorbed MO dye molecules [30]. In this regard, the pre-functionalization of the HNTs to ensure the electrostatic attachment of the pre-formed Au NPs has been proved as an efficient synthesis strategy to tune the size, dispersion and loading degree of the gold active phase on catalytic supports [31].

Additional time-dependence MO degradation experiments with the most active photo-catalytic Au-HNT sample were carried out under visible light (532 nm) at the maximum irradiation intensities (2 W). Fig. 2 shows the decay of the MO content after 4 consecutive irradiation cycles (1 h each) in the presence of 0.5 g L^{-1} of catalyst and in comparison with two blank experiments without Au-HNTs. The temperature was measured during the laser heating experiments in the presence of the catalyst with the aid of an external thermocouple. A maximum temperature of 32 °C corresponding to the thermal energy released to the aqueous media was detected. This temperature was used as a reference to measure the MO degradation in the absence of catalyst but no significant conversions could be detected (Fig. 2).

The low degradation rate observed further corroborates that the thermally-driven plasmonic effect must take place nearby the surface of the Au NPs at local levels. Different concentrations of catalyst (up to 2 g L^{-1}) at similar reaction times and laser intensities were evaluated and rendered pseudo-first order rate constants of 0.003 min^{-1}. This catalytic activity improved previous plasmon-assisted MO degradation experiments with Au/TiO_2 probably due to the distribution of Au in the catalytic support [32]. Consequently, the use of gold nanoparticles as plasmonic catalyst can be further extended to a wide variety of processes with environmental interest and to the challenging synthesis of selective chemicals. Furthermore, gold contrasts with other metals such as silver that has been recently related with multiple environmental and biological concerns.

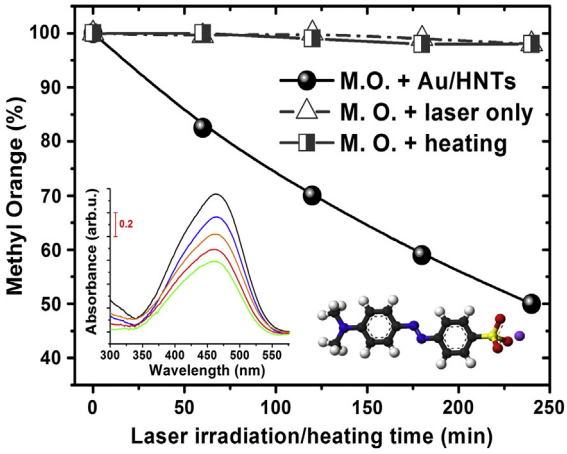

Fig. 2. Time-dependence degradation of MO in the presence of Au-2 wt.% loaded HNTs (solid spheres) and comparison with the same conditions without the catalyst after laser exposure (triangles) and heating at 32 °C (squares). Insets: MO absorbance band evolution with cumulative irradiation times and chemical structure of the targeted organic dye.

The Au-HNTs were finally characterized after reaction and despite partial aggregation contributing to a certain broadening of the SPR band (see SI for TEM and UV–Vis characterization), it becomes clear that the presence of THPC as stabilizer for Au and the amino-functionalization of the HNTs to improve the electrostatic attraction are extremely positive. These interactions further ensure the stability of the photo-catalyst and minimize the migration, aggregation and/or leaching of the noble-metal NPs that keep similar mean sizes and particle distributions (see Figure S1) [31]. Moreover, the use of HNTs represents an appealing alternative as catalytic support, given its world-wide availability as natural clay, its proven capacity for loading and adsorption of molecules and its alumino-silicate composition for functionalization with silane groups [33–35]. Hence, a potential application for reactions involving acidic centers can be also envisioned as recently shown by Scaiano and co-workers [26].

3. Conclusions

The electrostatic interactions between pre-synthesized Au NPs and amino-functionalized halloysite nanotubes have been successfully tested as an efficient and rational approach for the design of stable and tunable Au-HNT catalysts with plasmon-mediated photo-catalytic activity in the degradation of a model organic contaminant. A good Au NP dispersion to ensure good contact between the noble-metal surface and the adsorbed dye molecules seems to be imperative to obtain photo-catalytic response and an excess of gold does not guarantee any conversion enhancement. The proposed mechanism for the photo-degradation of MO involves a locally induced thermal heating induced by the SPR absorption of the incident visible light. HNTs are also presented as novel catalytic support with proper composition, morphology and stability for great potential for multiple plasmon-mediated reactions.

Acknowledgments

This research was supported in part by National Science Foundation Award No. CBET-0854118. This work has been also supported thanks to the Spanish Ministry of Science and Innovation (MICINN) with the abroad research stay granted to LG (grant EEBB-I-13-06033). Financial

support from MINECO (MAT2011-24988 grant, Spain), the European Research Council (ERC-Advanced Grant HECTOR) (267626) and CIBER-BBN (financed by the Instituto de Salud Carlos III with assistance from the European Regional Development Fund) is gratefully acknowledged. The microscopy work was conducted at the Laboratorio de Microscopias Avanzadas at Instituto de Nanociencia de Aragon—Universidad de Zaragoza. The authors acknowledge LMA-INA for offering access to their instruments and expertise. JLH acknowledges a Juan de la Cierva Postdoctoral Fellowship and a Marie Curie Reintegration Grant (CIG-NANOLIGHT).

Appendix A. Supplementary data

Supplementary data to this article can be found online at http://dx.doi.org/10.1016/j.catcom.2014.07.017.

References

[1] A. Kubacka, M. Fernandez-Garcia, G. Colon, Chem. Rev. 112 (2012) 1555–1614.
[2] M.C. Ortega-Liebana, E. Sanchez-Lopez, J. Hidalgo-Carrillo, A. Marinas, J.M. Marinas, F.J. Urbano, Appl. Catal. B Environ. 127 (2012) 316–322.
[3] A. Primo, A. Corma, H. Garcia, Phys. Chem. Chem. Phys. 13 (2011) 886–910.
[4] K. Awazu, M. Fujimaki, C. Rockstuhl, J. Tominaga, H. Murakami, Y. Ohki, N. Yoshida, T. Watanabe, J. Am. Chem. Soc. 130 (2008) 1676–1680.
[5] S. Sarina, E.R. Waclawik, H.Y. Zhu, Green Chem. 15 (2013) 1814–1833.
[6] X.M. Zhou, G. Liu, J.G. Yu, W.H. Fan, J. Mater. Chem. 22 (2012) 21337–21354.
[7] W.B. Hou, S.B. Cronin, Adv. Funct. Mater. 23 (2013) 1612–1619.
[8] C. Novo, A.M. Funston, P. Mulvaney, Nat. Nanotechnol. 3 (2008) 598–602.
[9] H.Y. Zhu, X. Chen, Z.F. Zheng, X.B. Ke, E. Jaatinen, J.C. Zhao, C. Guo, T.F. Xie, D.J. Wang, Chem. Commun. (2009) 7524–7526.
[10] X. Chen, Z.F. Zheng, X.B. Ke, E. Jaatinen, T.F. Xie, D.J. Wang, C. Guo, J.C. Zhao, H.Y. Zhu, Green Chem. 12 (2010) 414–419.
[11] M.D. Xiao, R.B. Jiang, F. Wang, C.H. Fang, J.F. Wang, J.C. Yu, J. Mater. Chem. A 1 (2013) 5790–5805.
[12] C.J.B. Alejo, C. Fasciani, M. Grenier, J.C. Netto-Ferreira, J.C. Scaiano, Catal. Sci. Technol. 1 (2011) 1506–1511.
[13] C. Fasciani, C.J.B. Alejo, M. Grenier, J.C. Netto-Ferreira, J.C. Scaiano, Org. Lett. 13 (2011) 204–207.
[14] J.C. Scaiano, K. Stamplecoskie, J. Phys. Chem. Lett. 4 (2013) 1177–1187.
[15] V. Myroshnychenko, J. Rodriguez-Fernandez, I. Pastoriza-Santos, A.M. Funston, C. Novo, P. Mulvaney, L.M. Liz-Marzan, F.J.G. de Abajo, Chem. Soc. Rev. 37 (2008) 1792–1805.
[16] J.R. Adleman, D.A. Boyd, D.G. Goodwin, D. Psaltis, Nano Lett. 9 (2009) 4417–4423.
[17] D.G. Duff, A. Baiker, P.P. Edwards, Langmuir 9 (1993) 2301–2309.
[18] J.L. Hueso, V. Sebastian, A. Mayoral, L. Uson, M. Arruebo, J. Santamaria, RSC Adv. 3 (2013) 10427–10433.
[19] M. Zieba, J.L. Hueso, M. Arruebo, G. Martinez, J. Santamaria, New J. Chem. (2014), http://dx.doi.org/10.1039/c3nj01127e.
[20] P. Yuan, P.D. Southon, Z.W. Liu, M.E.R. Green, J.M. Hook, S.J. Antill, C.J. Kepert, J. Phys. Chem. C 112 (2008) 15742–15751.
[21] A.B.S. Bakhtiari, D. Hsiao, G.X. Jin, B.D. Gates, N.R. Branda, Angew. Chem. Int. Edit. 48 (2009) 4166–4169.
[22] W.H. Hung, M. Aykol, D. Valley, W.B. Hou, S.B. Cronin, Nano Lett. 10 (2010) 1314–1318.
[23] M. Gonzalez-Bejar, K. Peters, G.L. Hallett-Tapley, M. Grenier, J.C. Scaiano, Chem. Commun. 49 (2013) 1732–1734.
[24] P. Christopher, H.L. Xin, S. Linic, Nat. Chem. 3 (2011) 467–472.
[25] S. Linic, P. Christopher, D.B. Ingram, Nat. Mater. 10 (2011) 911–921.
[26] G.L. Hallett-Tapley, M.J. Silvero, C.J. Bueno-Alejo, M. Gonzalez-Bejar, C.D. McTiernan, M. Grenier, J.C. Netto-Ferreira, J.C. Scaiano, J. Phys. Chem. C 117 (2013) 12279–12288.
[27] X. Chen, H.Y. Zhu, J.C. Zhao, Z.T. Zheng, X.P. Gao, Angew. Chem. Int. Edit. 47 (2008) 5353–5356.
[28] N.L. Pacioni, M. Gonzalez-Bejar, E. Alarcon, K.L. McGilvray, J.C. Scaiano, J. Am. Chem. Soc. 132 (2010) 6298–6299.
[29] S.M. Sun, W.Z. Wang, L. Zhang, M. Shang, L. Wang, Catal. Commun. 11 (2009) 290–293.
[30] N. Weiher, E. Bus, L. Delannoy, C. Louis, D.E. Ramaker, J.T. Miller, J.A. van Bokhoven, J. Catal. 240 (2006) 100–107.
[31] C.J. Jia, F. Schuth, Phys. Chem. Chem. Phys. 13 (2011) 2457–2487.
[32] W.B. Hou, Z.W. Liu, P. Pavaskar, W.H. Hung, S.B. Cronin, J. Catal. 277 (2011) 149–153.
[33] E. Abdullayev, R. Price, D. Shchukin, Y. Lvov, ACS Appl. Mater. Interfaces 1 (2009) 1437–1443.
[34] S. Barrientos-Ramirez, G.M. de Oca-Ramirez, E.V. Ramos-Fernandez, A. Sepulveda-Escribano, M.M. Pastor-Blas, A. Gonzalez-Montiel, Appl. Catal. A Gen. 406 (2011) 22–33.
[35] Y.M. Lvov, D.G. Shchukin, H. Mohwald, R.R. Price, ACS Nano 2 (2008) 814–820.